ELSEVIER

Polymer 41 (2000) 8349–8354

polymer

www.elsevier.nl/locate/polymer

Atomic detail simulation studies of unsubstituted and substituted poly(*p*-phenylene terephthalate)s

T. Launne[a,*], I. Neelov[a,b], F. Sundholm[a]

[a]*Laboratory of Polymer Chemistry, University of Helsinki, PB-55, FIN-00014 Helsinki, Finland*
[b]*Institute of Macromolecular Compounds, Russian Academy of Sciences, Bolshoi pr. 31, V. O., St. Petersburg, Russia*

Received 12 January 2000; accepted 24 March 2000

Abstract

Results of computer simulations of poly(*p*-phenylene terephthalate) (PPT) and 1,4-phenylene-2-octyloxy terephthalate (PTA8) are presented. The structures obtained from the *NPT* dynamics simulations were studied and compared at an atomistic level, at four different temperatures: 300, 450, 575 and 625 K. The side chains of PTA8 force the aromatic units into a planar orientation instead of the staggered structure of PPT. The planar orientation causes the decreasing of the strong non-bonded interactions between the neighbouring main chains. Additionally, it enables the regular staggered arrangement of the main chains in a stack of chains in order to get better packing. The staggered structure of the aromatic units remains at all temperatures for PPT. In the case of PTA8, the orientation gets more or less random as a function of temperature. Both polymers, PPT and PTA8, are relatively extended, but the end-to-end distances of PTA8 decrease ~4 Å as the temperature is raised from 300 to 625 K. The dihedral distribution of the side chains gets random as the temperature increases.

Keywords: Aromatic polyester; Substitution; Modelling

1. Introduction

Liquid crystalline polymers with mesogenic groups in the main chain have been studied extensively because of their capability to form high-strength fibres. A serious problem encountered when investigating and processing these materials is their extremely low solubility and high melting temperature often being located above the limits of thermal stability. Incorporation of flexible side chains into the structure of such polymers has been proven to be an effective method to increase the solubility in common solvents and decrease the melting temperature [1–8]. Poly(*p*-phenylene terephthalate) (PPT) is an aromatic polyester that has a melting point at 600°C, as measured by differential scanning calorimetry at a heating rate of 80°C/min to minimize degradation [9]. The side chains have been monosubstituted or disubstituted either to the hydroquinone moiety or to the terephthalic acid moiety of PPT.

A number of molecular modelling efforts have been carried out on thermotropic liquid crystalline polymers in order to gain insight into the structural organization. The atomistic modelling techniques give us a possibility for a better understanding of structure–property relationship of polymers at an atomistic level. Usually, the molecular modelling techniques are combined with X-ray diffraction measurements in order to solve the crystalline structure at room temperature. Atomic-detail simulations of smectic and nematic liquid crystals have been performed by Monte Carlo and molecular dynamics simulations [10–18]. Biswas and Schurmann [19] studied the extent of order in the side chains of wholly aromatic polyesters containing two and four hexadecyloxy side chains, but no more detailed analysis of the effect of the substitution to the behaviour of the aromatic polyesters have been reported earlier.

In our previous article, we reported the study of the monomer units with molecular mechanics calculations and single chains with the Metropolis Monte Carlo method [20]. Now, we have taken into account the effect of the neighbouring molecules by using periodic simulation boxes. In our latest study, we have done molecular dynamics simulations of material cells of PPT and 1,4-phenylene terephthalate with an octyloxy side chain (PTA8), see Fig. 1 [21]. The average initial structure for the simulations was taken from the experimental X-ray spectra. There are several experimental studies that indicate that the monosubstituted stiff polymer forms "double stacks" with back-to-back array of the main chains (Fig. 2) [3,5,22]. In our simulations it was

* Corresponding author. Tel.: +358-0-1911.
E-mail address: launne@csc.fi (T. Launne).

0032-3861/00/$ - see front matter
PII: S0032-3861(00)00246-9

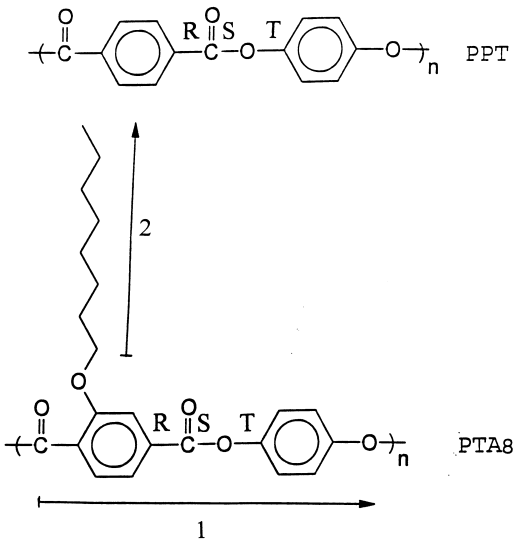

Fig. 1. Repeating units of PPT and PTA8.

possible to predict the crystal → layered liquid crystal phase transition temperature (T_m) for PTA8 by plotting the specific volumes as a function of temperature. The resulting mesophase showed the existence of a layered nematic phase, which was consistent with the experimental findings. The outline of this article is to study the structures of PPT and PTA8 at different temperatures in more detail. Additionally, the structures of PTA8 are studied at a crystalline state and at a liquid crystalline state and the phase transition was obtained at the microscopic level.

2. Simulation methodology

All calculations were done using the InsightII (version 400P) of Molecular Simulations Inc. (MSI) [23]. The new Compass (condensed-phase optimized molecular potentials for atomistic simulations) forcefield of MSI was used [24–26].

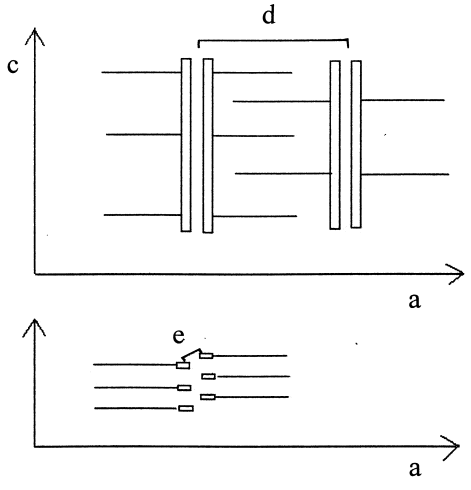

Fig. 2. Schematic illustration of monosubstituted hairy rod polymers.

The simulation boxes consisted of 18 (PPT) and 16 (PTA8) chains of nine monomer units. Trajectories obtained from constant pressure and temperature (*NPT*) simulations at 300, 450, 575 and 625 K were used in the structural analyses. All simulations were performed at atmospheric pressure (0.1 MPa) and time-step was 0.5 fs. The full details of the force-field testing and simulation procedure have been described elsewhere [21].

3. Results and discussion

3.1. Dihedral angle distributions

The conformational behaviour of the molecules was characterized by the distributions of the dihedral angles. The dihedral angle distributions of (*R*, *S*, *T*) at 300, 450, 575 and 625 K are shown in Figs. 3 and 4 for PPT and PTA8, respectively. The definitions of these dihedral angles are shown in Fig. 1. Although PTA8 is asymmetrically monosubstituted, the dihedral angle distributions of the neighbouring ester bonds were relatively similar. Therefore, the distributions of both ester group torsion angles are included in these plots.

As mentioned in our previous article, rotation around the *S* bond introduces kinks into the chain and hence it is important from the viewpoints of liquid crystalline behaviour and processability. It can be seen from Figs. 3 and 4 that there is no appearance of *gauche* states at any temperature in either polymer PPT or PTA8. This is expected due to low probability of *gauche* states; even at 625 K the probability is only 0.15% for PPT and 0.80% for PTA8 according to the Boltzmann factor [20]. Additionally, the transition from *trans* to *gauche* state would require exceeding a relatively high *trans–gauche* energy barrier, which is 10 kcal/mol for PPT and 8 kcal/mol for PTA8, respectively. However, the shape of the *trans* distribution becomes broader at higher temperatures. This effect is more strong in the case of PTA8 compared to PPT. This indicates that PTA8 is a more flexible polymer due to larger librations near the *trans* minimum area.

The dihedral angle *T* affects the orientation of the planes of the aromatic units relative to each other. As Hanna et al [27] determined in their X-ray diffraction and molecular simulation studies, the crystal packing of PPT favours intermolecular phenyl-edge to phenyl-face and carbonyl-carbon to carbonyl-oxygen interactions over other possibilities. This was seen also in our MD simulations; the molecules prefer the conformations where the hydroquinone rings are twisted relative to the rigid terephthalic acid part of the molecule and the orientation of the molecules favour the phenyl-edge to phenyl-face interactions. Despite the low intramolecular rotational barrier (<2 kcal/mol), no rotations around the *T* bond are seen in the case of PPT. This is due to strong non-bonded interactions between the neighbouring chains. On the contrary, a similar packing mode is not

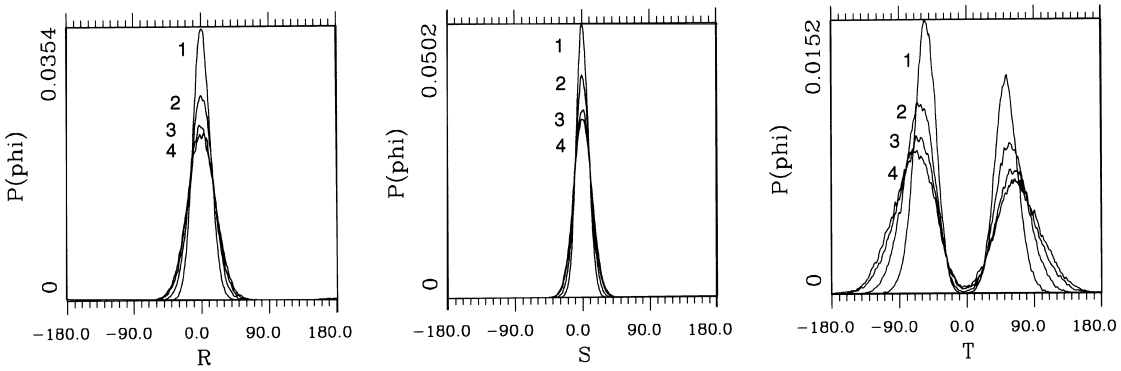

Fig. 3. Distributions of the dihedral angles (*R, S, T*) of PPT at: (1) 300 K; (2) 450 K; (3) 575 K; and (4) 625 K.

seen in the case of PTA8. At room temperature the *T* dihedral angles are at *trans* state indicating that the aromatic units are in the same plane instead of the staggered structure of PPT. Additionally, as the temperature increases the orientation gets more or less random. Because the rotational barrier of *T* in PTA8 is the same as for PPT, the reason for different behaviour in the bulk state must be in the non-bonded interactions. The side chains "force" the planes of the aromatic units to orient into a planar structure instead of the staggered structure of PPT. Due to the low rotational barrier of the *T* bond, rotation around this bond is the most susceptible to the perturbation by intermolecular packing forces. Additionally, as the strong intermolecular phenyl-edge to phenyl-face and carbonyl-carbon to carbonyl-oxygen interactions decrease, the relative orientation of the aromatic units also begins to fluctuate at higher temperatures disrupting the most efficient packing mode of PTA8.

The *T* bond may be responsible also for the "gliding" of the chains along the main chain direction with respect to each other. As mentioned earlier, the average initial structure for the simulations of PTA8 were taken from the experimental X-ray diffraction spectra (see Fig. 2). The cell angles of the periodic box were initially 90° before any optimization procedures. After the minimization, the cell angle between cell edges c and b increased drastically to ~145°. This value remained relatively unchanged during the *NPT* simulations. The reason for this kind of behaviour may be in the planar orientation of the aromatic units, which in turn is affected by *T*. As the strong non-bonded interactions between the aromatic rings decrease due the substitution, they enable the regular staggered arrangement of the main chains in a stack of chains in order to get better packing. The schematic illustration of the array of polymer chains is shown in Fig. 5. A similar kind of phenomenon was also found by Kricheldorf et al. [28], who studied the chiral sanidic polyesters derived from 2,5-bis(alkylthio)-terephthalic acids. They concluded that the reason for the staggered arrangement within the layers was due to the large volume required of the sulphur atoms and the attached side chains.

According to our previous molecular mechanics calculations, the *trans–cis* rotational barrier of the *R* bond is so high (~5 kcal/mol) in the case of PPT that the average population of these states does not change as the temperature increases at least up to $T = 625$ K. Only the distributions around the *trans* state get wider as the temperature increases. However, the substitution decreases the *trans–cis* barrier to ~4 kcal/mol, which means that the rotation around the *R* bond is essentially less hindered at high temperatures. This can be clearly seen from Fig. 4, where the population of *cis* conformations of PTA8 increases as a function of temperature. The reason for this kind of

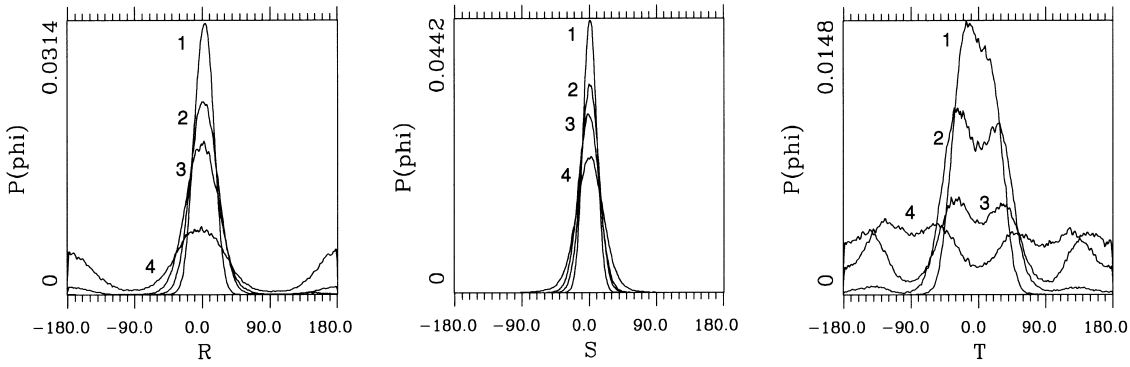

Fig. 4. Distributions of the dihedral angles (*R, S, T*) of PTA8 at: (1) 300 K; (2) 450 K; (3) 575 K; and (4) 625 K.

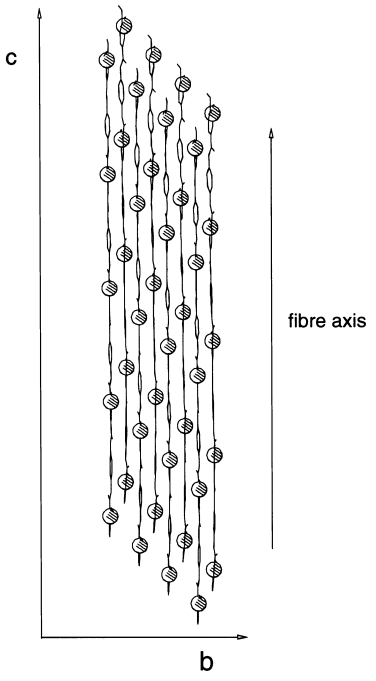

Fig. 5. Schematic illustration of the array of polymer chains in a stack of main chains. Oxygen atoms connecting the main chains and the side chains are marked with circles.

behaviour can be partly in the intermolecular interactions, in addition to the intramolecular behaviour. This is confirmed by the fact that there is no large difference between the distributions of the two neighbouring *R* torsion angles, although the substitution decreases the rotational barrier of only the other *R* bond. The packing of the chains has been disrupted due to rotation of the *T* bond, see above, which may facilitate also the rotation around the *R* bond. The appearance of *cis* conformations decrease slightly the end-to-end distance of the chain, as is shown schematically in Fig. 6.

The dihedral angle distributions of the side chains are

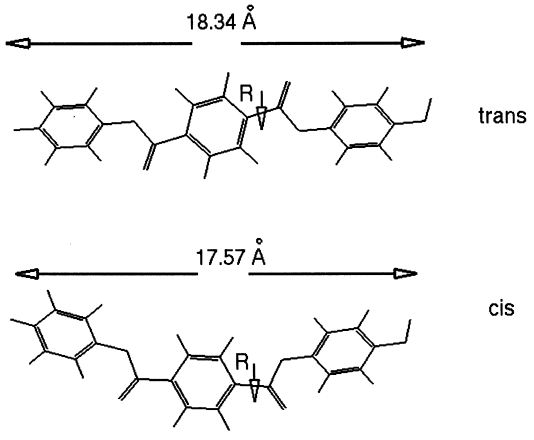

Fig. 6. Repeating unit of PPT. Comparison of *trans* and *cis* conformations of *R*.

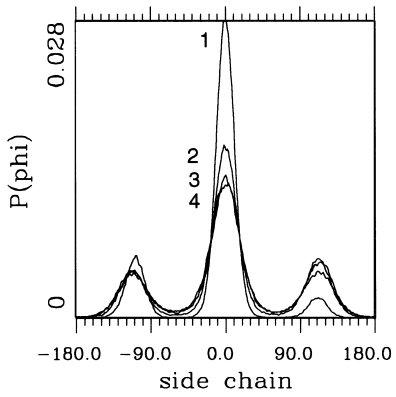

Fig. 7. Distributions of the side chain dihedral angles of PTA8 at: (1) 300 K; (2) 450 K; (3) 575 K; and (4) 625 K.

shown in Fig. 7. At room temperature the side chains are highly extended. At 300 K the probability of the *trans* state is about seven times greater than the probability of the *gauche* state. However, the population of the *gauche* states is clearly increased at higher temperatures. At the highest temperature (625 K) the probability for *trans* state is only about three times larger than for a *gauche* state. By calculating the orientational order of the side chain, it was also possible to see that the orientation of the side chains gets more or less random at 575 and 625 K, see Fig. 8. The ordering of the main chains and the side chains were calculated as a function of temperature for the final structures of each simulation. The orientational order *S* in the system was quantified by diagonalizing the order tensor, defined as

$$Q_{\alpha\beta} = \frac{1}{N}\sum_{i=1}^{N}\frac{1}{2}(3u_{i\alpha}u_{i\beta} - \delta_{\alpha\beta}) \quad (1)$$

where $u_{i\alpha}$ is the α component ($\alpha = x, y, z$) of the vector along the monomer unit of the main chain (1) and the end-to-end vector of the side chain (2), see Fig. 1; N is the corresponding number of such units and $\delta_{\alpha\beta}$ is the Kronecker delta. As it can be seen from Fig. 8, the side chains are relatively well-ordered crystalline state, but the ordering decreases drastically at 575 and 625 K. The order parameter *S* of the main chains is close to 1 at all temperatures. However, a small drop between 575 and 625 K indicating a decrease in ordering may be explained by the strong increase of the *cis* states of the *R* dihedral angle. The "bending" of the main chains could disrupt the efficient packing mode of the system.

3.2. The end-to-end distances

The average end-to-end distances were calculated for PPT and PTA8. The end-to-end distances of PPT remained relatively unchanged (~53 Å) at all temperatures, which was expected. There is no change in the average population of the torsion angles *R* and *S*, which affects the end-to-end distance of the main chain. However, larger changes could be seen in the case of PTA8, see Fig. 9. This can be

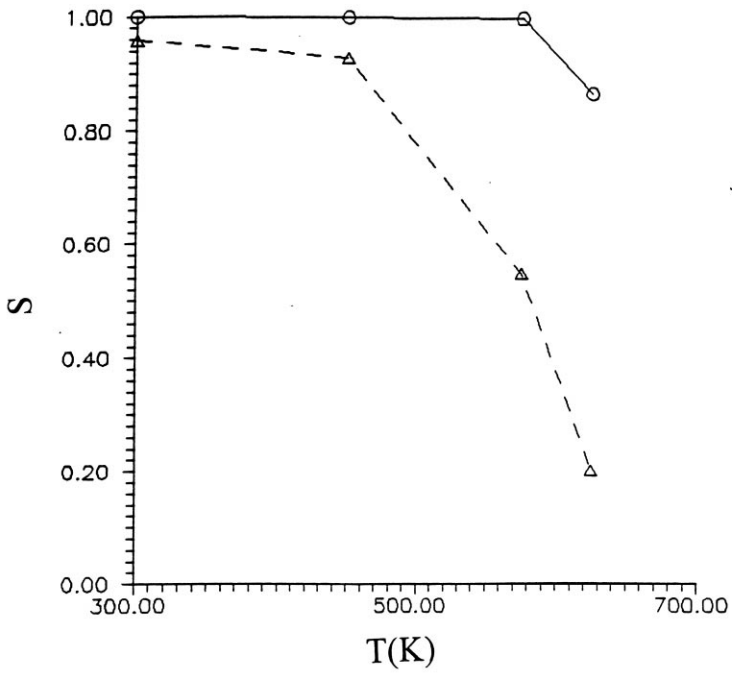

Fig. 8. Orientational order parameter *S* for the main chain (—) and the side chain (– – –) as a function of temperature.

explained by the behaviour of dihedral angles *R* and *S*. Distribution of dihedral *R* in Fig. 4 shows a great increase of *cis* conformations at 625 K, which influences the end-to-end distance in way described above (see Fig. 6). Additionally, the distribution of *trans* states of *S* gets wider as the temperature increases decreasing the average end-to-end distances of PTA8.

3.3. X-ray diffraction simulations

The X-ray diffraction patterns of PTA8 were calculated in order to get an overall description of the ordering of the system, see Fig. 10. The diffraction spectra were calculated for the last structures of each simulation. The strong reflection at $2\theta \sim 4$ (22 Å) indicated that the layered structure exists in the crystalline state. This peak remains at all temperatures, including the mesophase temperatures 575 and 625 K. This means the existence of a layered nematic mesophase. The reflection at $2\theta \sim 12$ (7.5 Å) is seen at a crystalline state only and very weakly at 575 K. This represents the *e* distance, see Fig. 2.

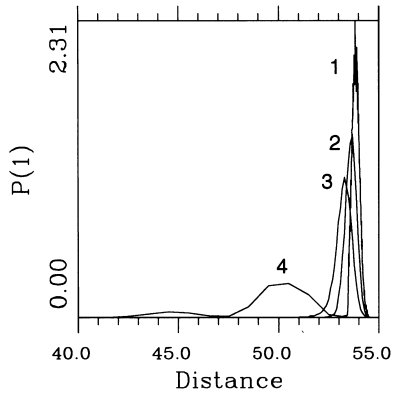

Fig. 9. The end-to-end distances of PTA8 chains at: (1) 300 K; (2) 450 K; (3) 575 K; and (4) 625 K.

4. Conclusions

The material cells of PPT and PTA8 were studied as a function of temperature by using *NPT* dynamics simulations. The structures were studied in more detail at 300, 450, 575 and 625 K. In the crystalline state, the side chains force the aromatic units into a planar structure instead of the staggered structure of PPT. Due to this, the strong phenyl-edge to phenyl-face and carbonyl-carbon to carbonyl-oxygen interactions decrease and the chains can form a staggered arrangement within a stack of main chains in order to get a better packing. Additionally, the orientation of the aromatic units gets random as the temperature increases. The end-to-end distances of PPT remained practically unchanged as a function of temperature, but the end-to-end distances of PTA8 slightly decreased (4 Å) when the temperature was raised from room temperature to 625 K. This was mainly due to the *cis* conformations of the *R* bonds.

The translational diffusion of the stiff chains would probably be so slow that the simulation of this kind of behaviour at the atomistic level would be perhaps too time-consuming at present. Therefore, we cannot be sure whether the simulation times are sufficient for the full structural reorganization, although the average energy and the density

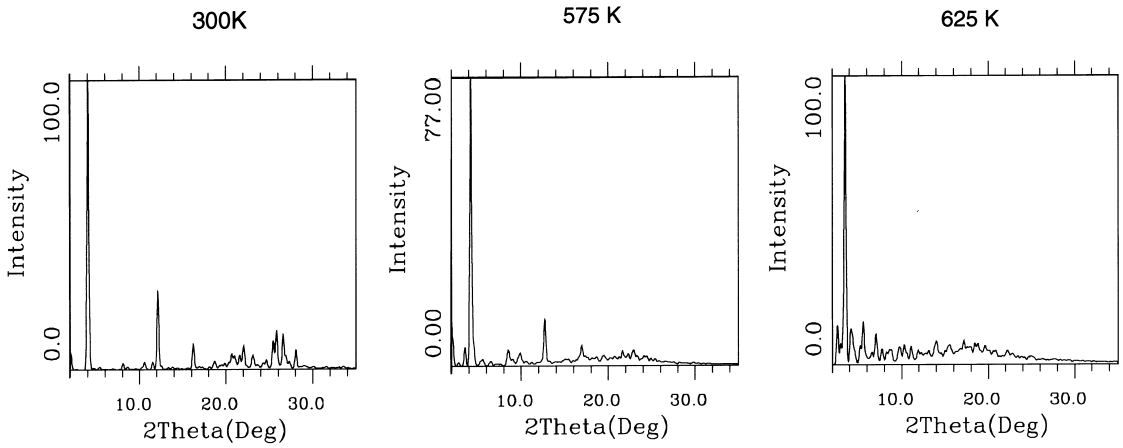

Fig. 10. Simulated X-ray diffraction patterns of PTA8 at 300, 450, 575 and 625 K.

equilibrations were reached. Instead, we have concentrated on the studies where the differences of PPT and PTA8 have been examined at the microscale as a function of temperature. Additionally, we have obtained the phase transition of PTA8 at the atomistic level. The reason for the lower phase transition temperature of PTA8 is naturally due to the large volume fraction of the flexible side chain in the system. Additionally, they decrease the intermolecular interactions between the neighbouring main chains. However, it is interesting to study how the substitution site effects the behaviour and the properties of the monosubstituted aromatic polyesters. The calculations where the alkoxy side chains are attached to the hydroquinone moiety instead of the terephthalic acid moiety are in progress and will be reported later.

Acknowledgements

The authors thank the Centre of Scientific Computing Ltd (CSC), Espoo, Finland for providing the computational resources, and the Academy of Finland for funding. The work is part of the European Science Foundation (ESF) SUPERNET programme.

References

[1] Herrmann-Schönherr O, Wendorff JH. Macromol Chem Rapid Commun 1986;7:791.
[2] Kricheldorf RH, Wulf DF. Polymer 1998;39:2683.
[3] Berger K, Ballauf M. Mol Cryst Liq Cryst Inc Nonlin Opt 1988;157:109.
[4] Cervinka L, Ballauf M. Colloid Polym Sci 1992;279:859.
[5] Kricheldorf HR, Domschke A. Macromolecules 1996;29:1337.
[6] Hyvärinen S. Licentiate thesis, University of Helsinki, Helsinki, 1997.
[7] Majnuz J, Catala JM, Lenz RW. Eur Polym J 1983;19:1043.
[8] Majnuz J, Lenz RW. J Polym Chem: Part A Polym Chem 1994;32:2775.
[9] Jackson Jr. WJ. Br Polym J 1997;12:1431.
[10] Wong S-K, Blackwell J. Polymer 1989;30:225.
[11] Ishaq M, Blackwell H, Chvalun SN. Polymer 1996;37:1765.
[12] Tsukruk V. Polymer 1992;33:2605.
[13] Jehnichen D, Friedel P, Bergmann J, Taut T, Tobisch J, Pospiech D. Polymer 1998;39:1095.
[14] Foulger SH, Rutledge GC. J Polym Sci: Part B Polym Phys 1998;36:727.
[15] Kitano Y, Usami I, Otama U, Okyama K, Jinda T. Polymer 1995;36:1123.
[16] Glaser MA, Malzbender R, Clark NA, Walba DM. Mol Simul 1995;14:343.
[17] Glaser MA, Malzbender R, Clark NA, Walba DM. J Phys: Condens Matter 1994;6:261.
[18] Bharadwaj RK, Boyd RH. Macromolecules 1998;31:7682.
[19] Biswas A, Schurmann BL. Polym Prepr 1992;33:562.
[20] Launne T, Neelov I, Sundholm F. Polymer 1999;40:2313.
[21] Unpublished results
[22] Lieser G. J Polym Sci Polym Phys Ed 1983;21:1611.
[23] InsightII User Guide, September 1996, San Diego: MSI 1996.
[24] Rigby D, Sun H, Eichinger BE. Polym Int 1997;44:311.
[25] Sun H, Rigby D. Spectrochim Acta, Part A 1997;53:1301.
[26] Sun H. J Phys Chem B 1998;102:7338.
[27] Hanna S, Coulter PD, Windle AH. J Chem Soc Faraday Trans 1995;91:2615.
[28] Kricheldorf HR, Wulff F, Wutz C. Macromol Chem Phys 1999;200:799.